# Supporting Information

## High-performance transparent and stretchable all-solid supercapacitors based on highly aligned carbon nanotube sheets

Tao Chen[1], Huisheng Peng[2], Michael Durstock[3], Liming Dai[1]*

[1]Center of Advanced Science and Engineering for Carbon (Case4Carbon), Department of Macromolecular Science and Engineering, Case Western Reserve University, 10900 Euclid Avenue, Cleveland, OH 44106 (USA). E-mail: liming.dai@case.edu.[2]State Key Laboratory of Molecular Engineering of Polymers, Department of Macromolecular Science and Laboratory of Advanced Materials, Fudan University, Shanghai 200438, China. [3]Materials and Manufacturing Directorate, Air Force Research Laboratory, RXBP, Wright-Patterson Air Force Base, OH 45433, USA

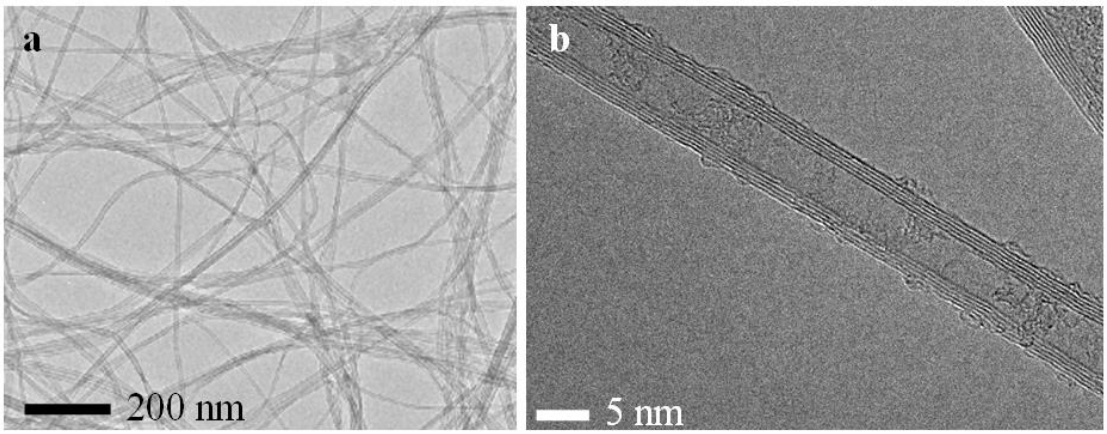


**Figure S1**. TEM images of the pristine carbon nanotubes from a vertically aligned CNT array.

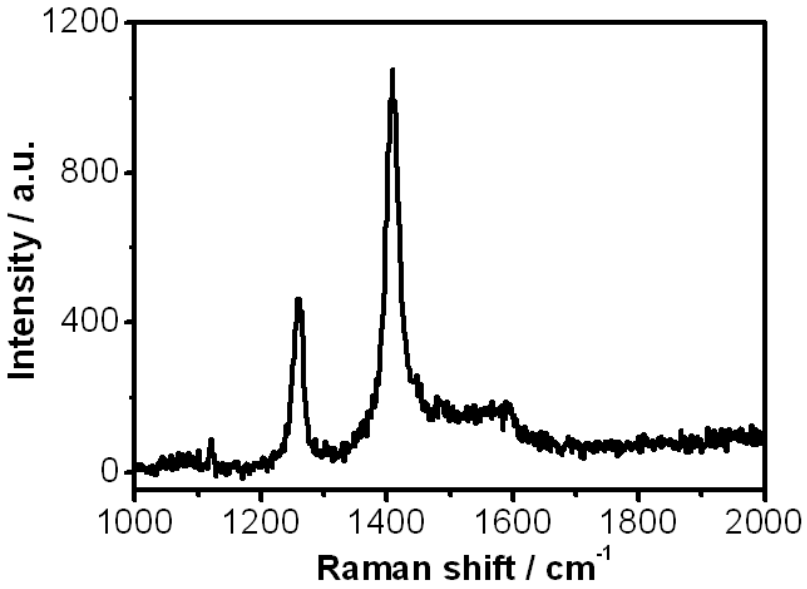


**Figure S2**. Raman spectrum of a horizontally aligned CNT sheet on the PDMS substrate.

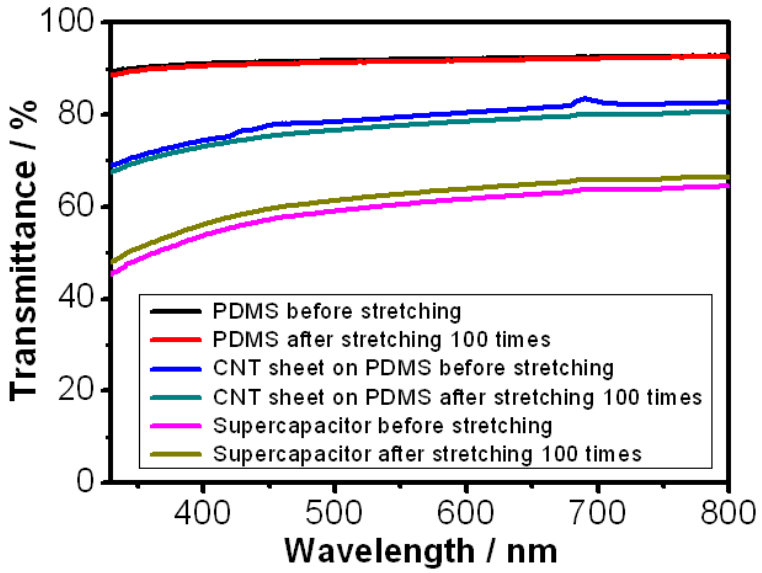


**Figure S3**. Transparencies of PDMS, one layer CNT sheet on the PDMS substrate, and supercapacitor based on electrodes with one layer CNT sheet on the PDMS substrate before and after having been stretched for 100 times.

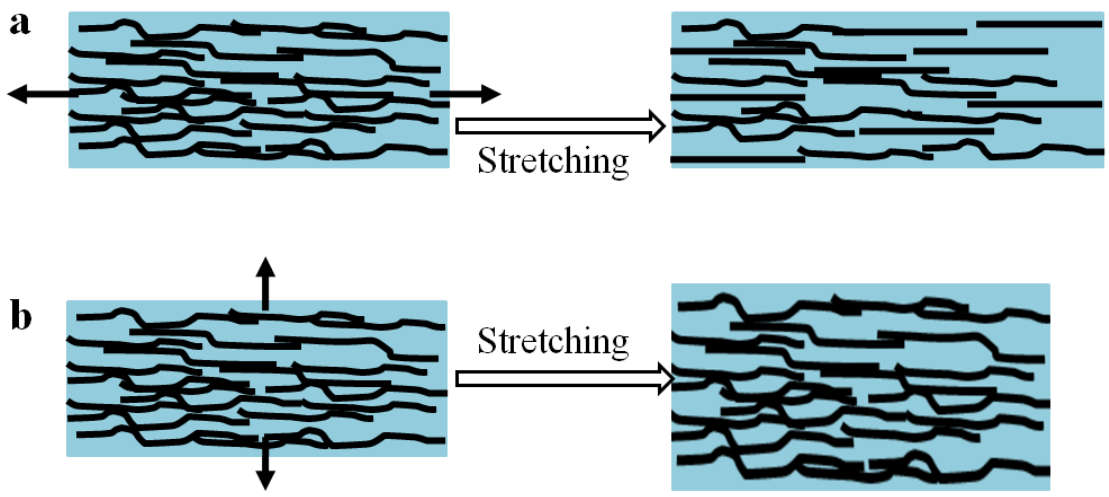


**Figure S4**. Schematic illumination of the aligned CNT sheet before and after stretching (a) along and (b) vertical to the nanotube length direction.

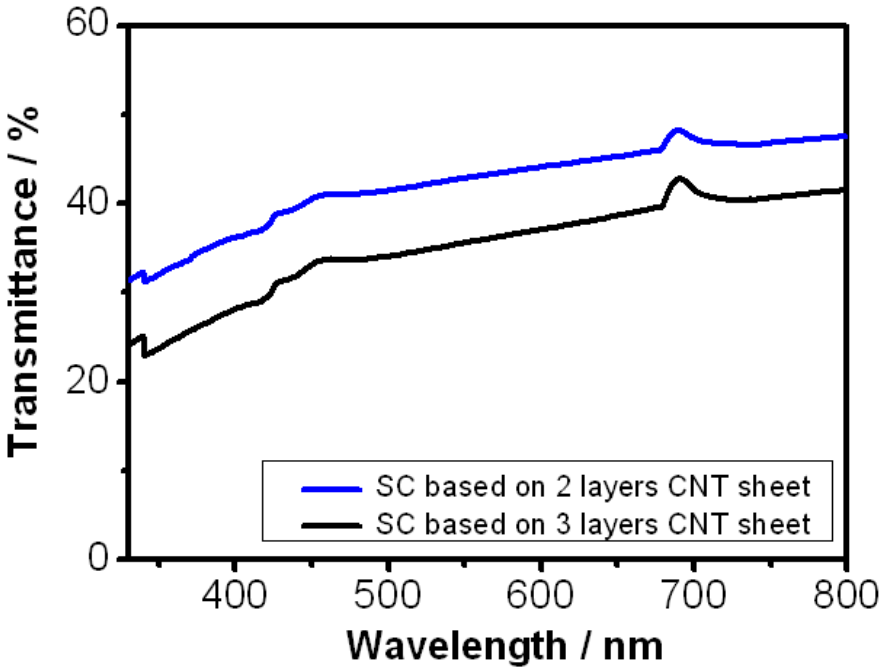


**Figure S5**. Transmittance spectra of the supercapacitors based on electrodes with two and three layers of CNT sheet on the PDMS substrate.

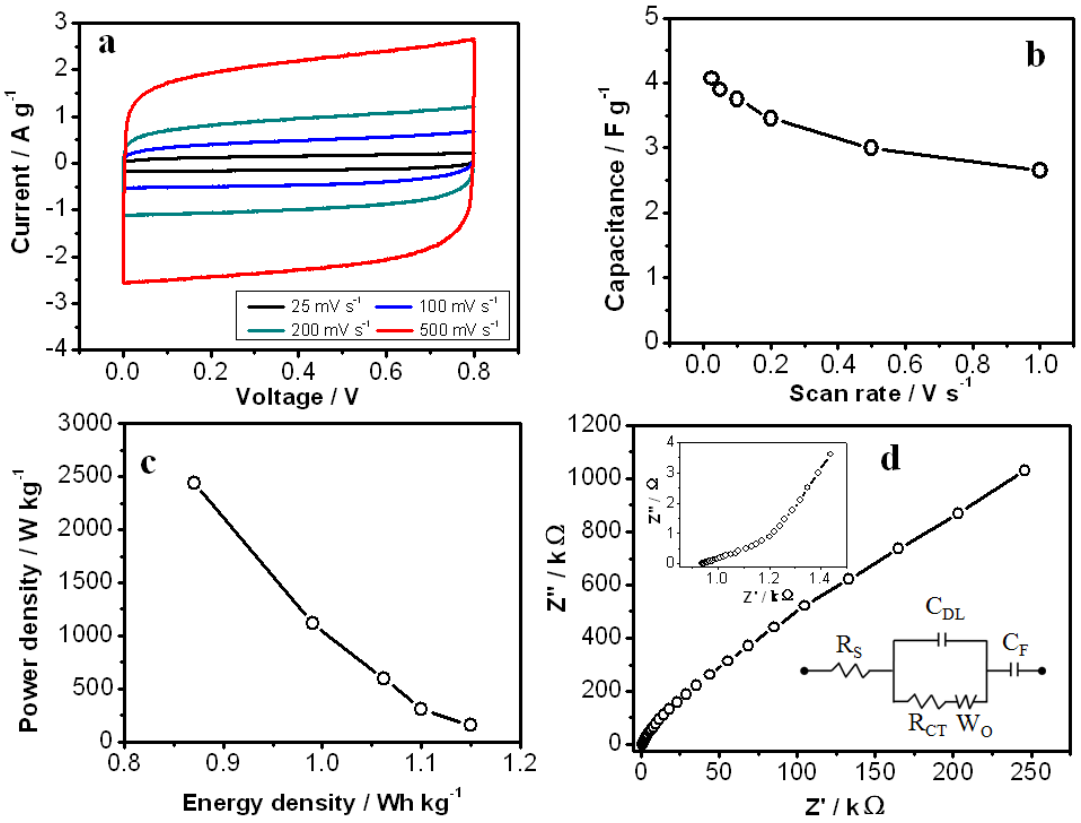


**Figure S6**. Electrochemical performance of the supercapacitor with a cross assembly configuration based on electrodes with one layer CNT sheet. (a) CV curves at different scanning rates and (b) Dependency of specific capacitance of supercapacitor on the scan rate. (c) Ragone plots of the supercapacitor and (d) Nyquist plots over the frequency range from $10^{-2}$ to $10^{5}$ Hz, the insets are the magnified view of the Nyquist curve and equivalent circuit, in which $R_S$ is the series resistance, $C_{DL}$ is double-layer capacitance, $R_{CT}$ is charge transfer resistance, $W_O$ is the Warburg diffusion element, and $C_F$ is the faradic capacitance.

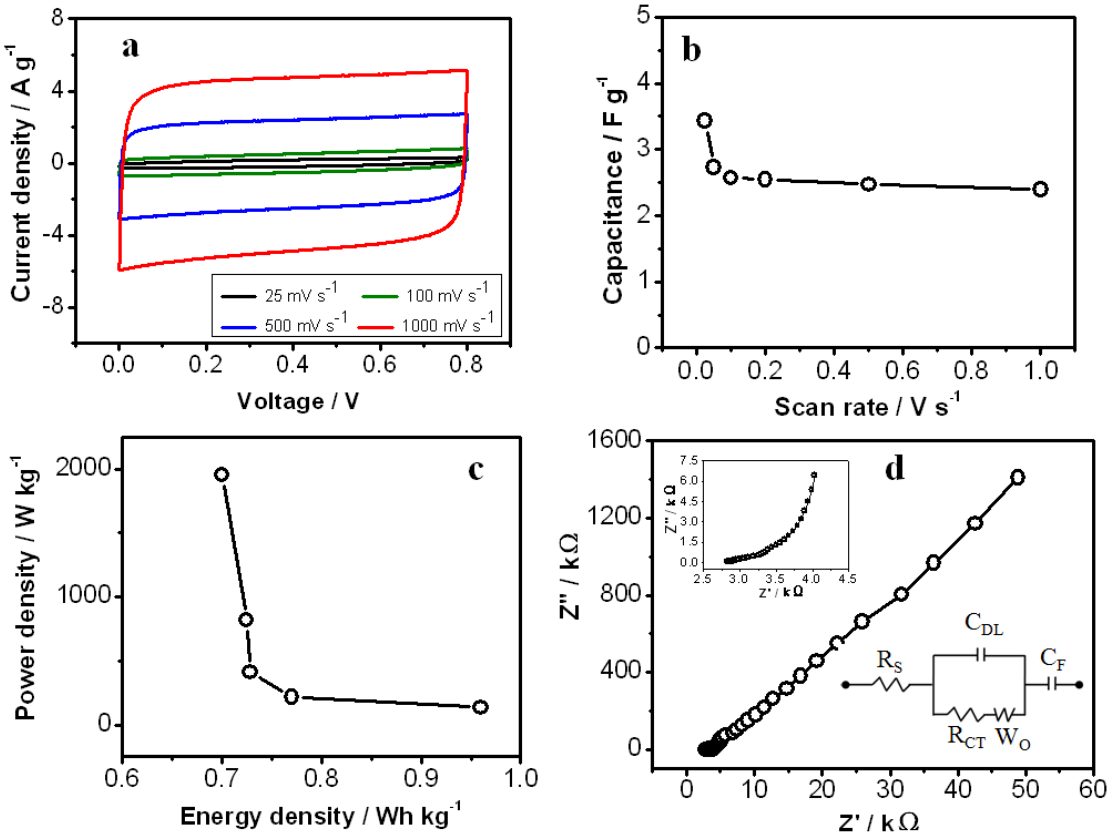


**Figure S7**. Electrochemical performance of the parallelly assembled supercapacitor based on electrodes with one layer CNT sheet. (a) CV curves at different scanning rate and (b) Dependency of specific capacitance of the supercapacitor on scan rates. (c) Ragone plots of the supercapacitor and (d) Nyquist plots over the frequency range from $10^{-2}$ to $10^{5}$ Hz, the insets are the magnified view of the Nyquist curve and equivalent circuit.

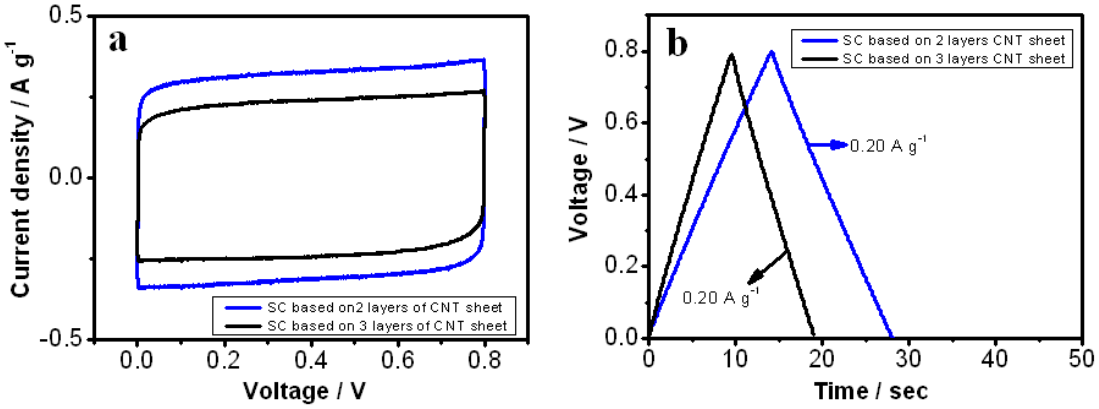


**Figure S8**. (a) CV curves at a scan rate of 0.1 V $s^{-1}$, and (b) galvanostatic charge-discharge curves of the assembled supercapacitors using electrodes with two and three layers of CNT sheet on the PDMS substrate.

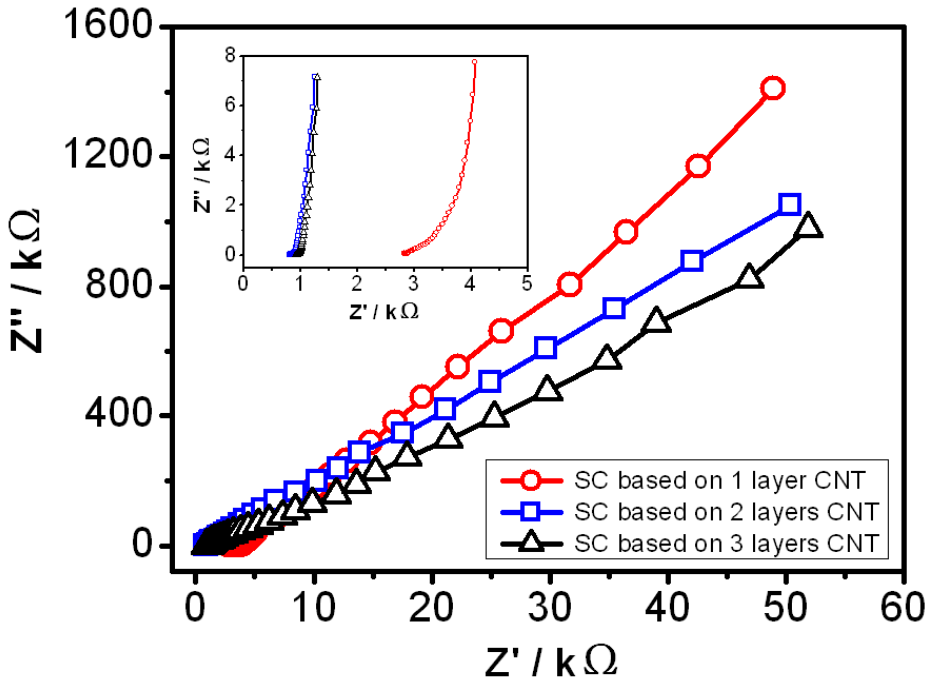


**Figure S9**. Nyquist plots of the supercapacitor based on the CNT electrodes with different layers of CNT sheet on the PDMS substrate over the frequency range from $10^{-2}$ to $10^{5}$ Hz.

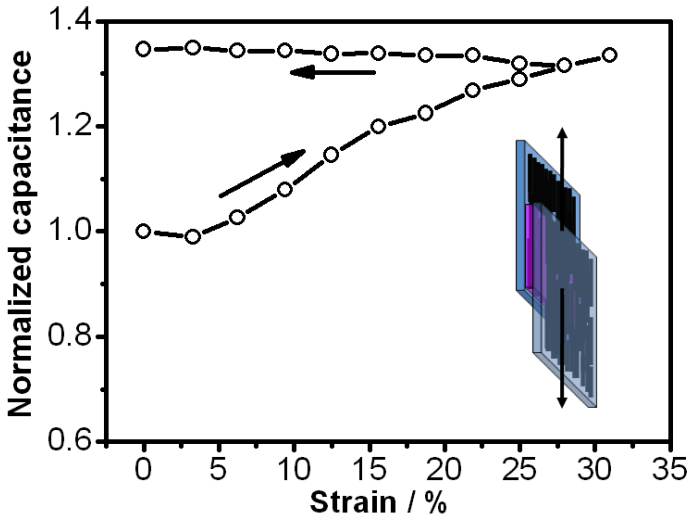


**Figure S10**. Normalized specific capacitance of the parallelly assembled supercapacitor as a function of the tensile strain as it was stretched at the first cycle along the nanotube length direction.

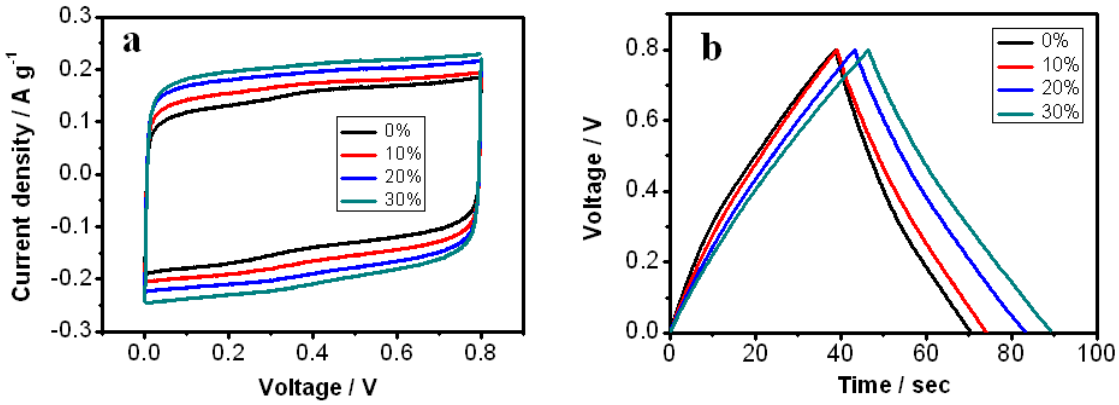


**Figure S11**. CV curves (at a scan rate of 0.1 V $s^{-1}$) and charge-discharge curves of the parallelly assembled supercapacitor with different stretching strains of 0 to 30% during the first stretching process.

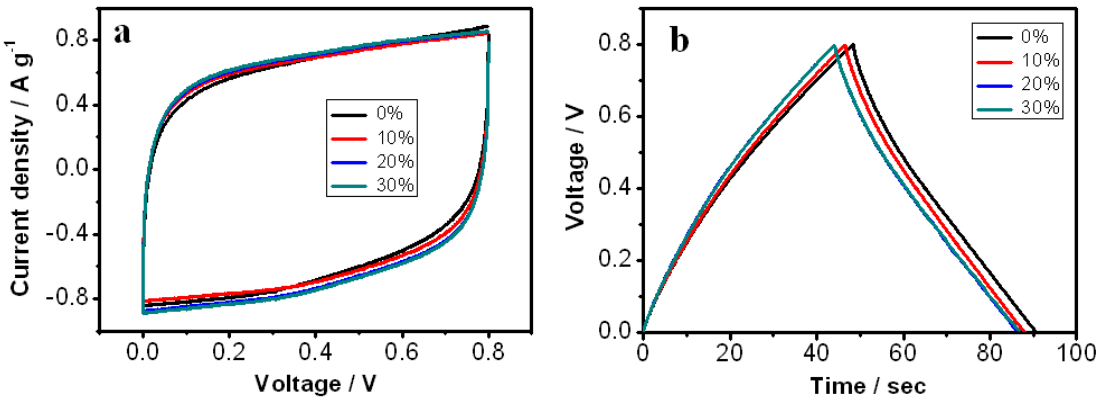


**Figure S12**. CV curves (at a scan rate of 0.1 V $s^{-1}$) and charge-discharge curves of the supercapacitor of a cross assembly configuration with different stretching strains of 0 to 30% during the first stretching process.